Pulse Radiolysis Study on the Estimation of Radiolytic Yields of Water Decomposition Products in High-Temperature and Supercritical Water: Use of Methyl Viologen as a Scavenger

Mingzhang Lin, Yosuke Katsumura,* Yusa Muroya, Hui He, Guozhong Wu,† Zhenhui Han, Toyoaki Miyazaki, and Hisaaki Kudo

Nuclear Engineering Research Laboratory, School of Engineering, The University of Tokyo, 2-22 Shirakata Shirane, Tokaimura, Nakagun, Ibaraki 319-1188, Japan

Received: March 15, 2004; In Final Form: July 28, 2004

In the present work, methyl viologen (1,1′-dimethyl-4,4′-bipyridinium dichloride) is used as a scavenger to estimate the radiolytic yields of water decomposition products from room temperature to 400 °C by pulse radiolysis method. $\{G(e_{aq}^-) + G(OH) + G(H)\}$ has been studied using a 0.5 mM MV^{2+} solution in the presence of 10 mM NaCOOH up to 200 °C and in the presence of 0.2 M ethanol up to 400 °C. The results show that the $\{G(e_{aq}^-) + G(OH) + G(H)\}$ increases with temperature up to 350 °C at 25 MPa, while it depends also on pressure in supercritical conditions. The $G(e_{aq}^-)$ was estimated using MV^{2+} solutions in the presence of 0.2 M *tert*-butyl alcohol. The results agree well with the reported data up to around 300 °C at 25 MPa; however, in supercritical conditions a very significant density effect was observed. At a given temperature, $G(e_{aq}^-)$ and $\{G(e_{aq}^-) + G(OH) + G(H)\}$ decrease with increasing density while at a fixed density they decrease with increasing temperature.

1. Introduction

For the last two decades, studies on supercritical water (SCW), or more generally supercritical fluids (SCF), have attracted considerable attention from chemists and engineers. The peculiar properties exhibited suggest many potential applications. As compared with water at room temperature, SCW has a much smaller dielectric constant ($\epsilon < 10$, similar to organic solvents), the hydrogen bond network is broken, and almost all its properties such as density, dielectric constant, p*K*w, and viscosity depend not only on temperature but also on pressure. Therefore SCW can be applied to the synthesis of functional materials as well as a 'green' solvent to completely destroy organic wastes such as PCB and dioxin, or chemical weapons. There are a number of review articles related to the recent research activities on supercritical water and fluids.[1−5]

Supercritical water has been also successfully applied in fossil power plants. In Japan, more than 20 power plants are being operated in supercritical conditions. Recently a new concept of nuclear reactor, a supercritical water-cooled reactor, has been proposed by Oka, et al.[6] This new concept reactor has advantages of higher thermal conversion efficiency, simplicity in structure, safety, etc. In these reactors, the same as in boiling water reactors (BWR) and pressurized water reactors (PWR), light water or heavy water is used not only as a coolant but also as a moderator. The water is exposed to a strong radiation field composed of γ-rays and 2-MeV fast neutrons, etc. As is well-known in the BWR and PWR, two radiolysis products of water, O_2 and H_2O_2, strongly affect the corrosion of the materials in the reactors. To mitigate the corrosion, H_2 gas or hydrazine is injected into the coolant to convert O_2 and H_2O_2 into water by radiolytic processes.

Computer simulation is usually required to help predict the concentrations of water decomposition products. However, to carry out this kind of simulation, knowledge of the temperature-dependent *G*-values (denoting the experimentally measured radiolytic yields) as well as of the rate constants of a set of reactions becomes very important. Therefore, intensive studies on water radiolysis up to a temperature of 300 °C were done in the last two decades, and sufficient data have been accumulated.[7−9] Computer simulation has been performed to help to understand the nature of the temperature dependence of *G* values.[10,11] The rate constants and *G*-values of the radiolysis of light and heavy water over the range 0−300 °C have been compiled by Elliot.[7,8] It is expected that a similar situation would also exist in the supercritical water-cooled nuclear reactors. Thus, fundamental studies on the radiation chemistry are indispensable. However, studies of the pulse radiolysis of supercritical water were not reported until 1998.[12,13] In recent years, a group at the Argonne National Laboratory and a group at the University of Tokyo simultaneously conducted two projects aimed at obtaining basic data on radiolysis of SCW. However, most of the studies were focused on the rate constants and spectral properties of transient species,[14−23] and few were concerned with the radiolytic yields of water decomposition products. One of the main difficulties was that the absorption spectra of transient species were usually temperature- and density-dependent but no data were available for the temperature-dependent absorption coefficients of the transient species studied.

In addition, although the absorption spectra of hydrated electrons have been measured up to 400 °C,[14] a direct measurement of the temperature-dependent spectra of some species such as the OH radical and the H atom is rather difficult, if not impossible. Therefore, to estimate *G* values, scavengers were usually introduced.[24,25] Among those scavengers that have been applied for the studies at elevated temperatures, methyl viologen (1,1′-dimethyl-4,4′-bipyridinium) was chosen for the present study, because it has advantages such as the high absorption

* Address correspondence to this author at the Nuclear Engineering Research Laboratory, School of Engineering, The University of Tokyo, Hongo 7−3−1, Bunkyo-ku, Tokyo 113, Japan (fax/ telephone: +81−3−5841−8624; email: katsu@q.t.u-tokyo.ac.jp).

† Present address: Institute of Applied Physics, P.O.Box 800-204, Shanghai, 201800, P.R. China.

10.1021/jp048854j CCC: $27.50
Published on Web 09/09/2004

coefficient of its cation radical $MV^{\bullet+}$, which we are interested in, and also fairly good thermal stability of this radical.

Moreover, as mentioned above, unlike water at room temperature or even at high temperature, many physicochemical properties under supercritical conditions are not only temperature dependent but also density dependent. As a matter of fact, it has been shown that reaction-rate constants and, qualitatively, the yield of hydrated electrons in SCW significantly depend on density.[22] Thus, it is of considerable interest to confirm the density effects on *G* values of water decomposition products other than the hydrated electrons and investigate them quantitatively.

2. Experiments

Experimental Setup, Chemicals, and Dose Measurement. In pulse radiolysis studies from room temperature to 300 °C, a quartz cell is normally employed. Above 300 °C, sapphire should be used in place of quartz because of the lower strength and higher solubility of quartz under the condition of supercritical water. Therefore, a specially designed irradiation cell made of Hastelloy HC22 with sapphire windows was constructed, which can be used up to 400 °C/40 MPa. The optical path length is 15 mm. The flow system is composed of a pump, a preheater, a heater, a backpressure regulator, and a power supply with a temperature control unit. Details of the apparatus were described elsewhere.[14] The flow rate was generally adjusted to 5−6 mL/min, corresponding to a residence time of about 5 s in the cell (the volume of the cell is about 0.6 cm^3). Fresh solutions prepared with Millipore filtered water (resistivity > 18.2 MΩ·cm) were used and the solutions were purged with argon or N_2O when necessary. In the case of alcohol as a scavenger, to compensate for the loss of alcohol after extensive gas purging, an appropriate amount of alcohol was added to the bulk solution every 2−3 h.

The conventional pulse radiolysis system installed at the Nuclear Engineering Research Laboratory, University of Tokyo, was used. The energy and pulse duration of the electron beam were 28 MeV and 2, 10, or 50 ns, respectively.

For the measurement of the rate constants of the reaction between MV^{2+} and hydrated electron, an experimental setup using two HPLC pumps was employed so that the initial concentration of MV^{2+} could be adjusted by changing the flow rate of the pumps. This allows us to measure the rate constant at a given temperature under the same beam conditions.

The dosimetry was done using the 10 mM KSCN dosimeter saturated with N_2O. A value of $G\epsilon((SCN)_2^{\bullet-}) = 5.2 \times 10^{-4}$ m^2/J at 475 nm was used.[26] The dose was normally adjusted between 20 and 60 Gy/pulse. The density of water is temperature dependent and it was assumed that the absorbed energy is proportional to the density. We could not measure the dose pulse by pulse because of the use of full-metal high-temperature cell, but the dose fluctuation is less than 5% during a daylong experiment.

Experimental Methods. As is well-known, after interaction with high-energy irradiation such as γ-rays, X-rays, or an electron beam, the water molecules are decomposed according to the scheme below:

$$H_2O \xrightarrow{\gamma,e^-} e_{aq}^-(2.63), H(0.55), OH(2.72), H_2(0.45), H_2O_2(0.68), HO_2(0.026) \quad (1)$$

The values in the parenthesis are of the primary yields in species/100 eV of water decomposition products at room temperature,[27] which are generally denoted by a symbol g(X) to distinguish them from the experimentally measured values *G*(Y).

In an aqueous solution containing MV^{2+} and formate ions $HCOO^-$, the following reactions take place[24,28−31]:

$$e_{aq}^- + MV^{2+} \rightarrow MV^{\bullet+} \quad k_2 = 8.3\times10^{10}\ M^{-1}s^{-1} \quad (2)$$

$$OH + HCOO^- \rightarrow COO^{\bullet-} + H_2O \quad k_3 = 3.2 \times 10^9\ M^{-1}s^{-1} \quad (3)$$

$$H + HCOO^- \rightarrow COO^{\bullet-} + H_2 \quad k_4 = 2.1 \times 10^8\ M^{-1}s^{-1} \quad (4)$$

The radical $COO^{\bullet-}$ can in turn reduce MV^{2+} to form $MV^{+\bullet}$:

$$COO^{\bullet-} + MV^{2+} \rightarrow MV^{\bullet+} + CO_2 \quad k_5 = 1 \times 10^{10}\ M^{-1}s^{-1} \quad (5)$$

The rate constants listed above are at room temperature.

Accordingly, the radiolytic yield of $MV^{\bullet+}$ should correspond to the total *G* value of the hydrated electron, the OH, and the H radical:

$$G(MV^{\bullet+}) = G(e_{aq}^-) + G(OH) + G(H) \quad (i)$$

But in case of an aqueous solution containing MV^{2+} and *tert*-butyl alcohol, H and the OH radical will be readily scavenged by *tert*-butyl alcohol (even if the H atom is not completely scavenged by *tert*-butyl alcohol, its reaction with MV^{2+} is to form a H adduct[32]); therefore only reaction 2 takes place, and

$$G(MV^{\bullet+}) = G(e_{aq}^-) \quad (ii)$$

At room temperature, $MV^{\bullet+}$ has a fairly strong absorption band located at $\lambda_{max} = 605$ nm with an absorption coefficient $\epsilon = 13\,100\ M^{-1}\ cm^{-1}$.[24] Therefore, measurements of the absorbance at 605 nm (A^T_{605nm}) at different temperatures allow us to estimate the *G* values of $MV^{\bullet+}$.

$$G(MV^{\bullet+}) = \frac{A^T_{605nm}}{\epsilon^T_{605nm} \times L \times \rho^T \times D \times 1.036 \times 10^{-7}} \quad (iii)$$

where ϵ^T_{605nm} and ρ^T are the absorption coefficient and density of water at temperature *T*; *L* and *D* represent the optical path of the high-temperature cell and the absorbed dose at room temperature, respectively.

3. Results and Discussion

3.1. Thermal Stability of Methyl Viologen in Aqueous Solution. Thermal stability of the scavenger(s) is essential for the studies at elevated temperatures. To obtain this information, a solution containing 25 μM MV^{2+} was passed through the high-temperature cell at different temperatures and different pressures, if necessary. The solution was collected at the exit of the backpressure regulator and measured by a UV−vis spectrometer within the range 200−300 nm (as shown in Figure 1); at room temperature an absorption band with $\lambda_{max} = 257$ nm can be observed. With increasing temperature, the shape of the spectrum and the absorbance at 257 nm does not change appreciably up to 300 °C. However, at 350 °C the absorbance decreases but the absorption peak almost does not change. At supercritical conditions the absorption band shifts to 240 nm, which has been assigned to mainly 4,4′-bipyridyl (BPY) and partly 1-methyl-4,4′-bipyridyl by the method of LC/MS (ESI cation mode), as shown in Scheme 1. Accordingly, it can be

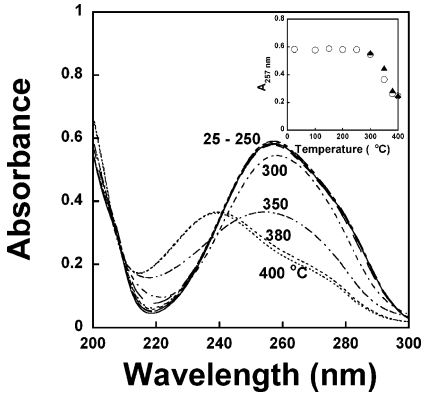

Figure 1. Absorption spectra of an aqueous solution containing 25 μM MV^{2+} measured after flowing through the high-temperature high-pressure cell at various temperatures with a constant pressure 25 MPa. Inset: the absorbance at 257 nm as a function of temperature, (○) flow rate = 2 mL/min.; (▲) 5 mL/min.

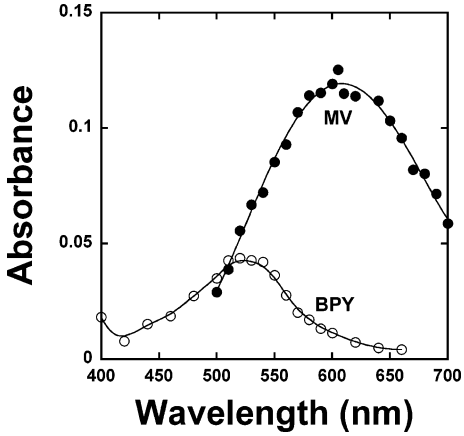

Figure 2. Transient absorption spectra obtained by pulse radiolysis of (●) 0.5 mM MV^{2+}/0.2 M *tert*-butyl alcohol and (○) 0.5 mM 4,4′-bipyridyl/0.2 M *tert*-butyl alcohol. Temperature: 400 °C; pressure: 30 MPa.

concluded that MV^{2+} is thermally stable up to at least 300 °C. It is noted that in the above method, where the solution was collected at the exit of the backpressure regulator, the heating time is longer than for the actual pulse radiolysis, where the residence time is about 5 s for a flow rate of 5−6 mL/min. Figure 2 shows the transient absorption spectra obtained by pulse radiolysis of a solution of 0.5 mM MV^{2+}/0.2 M *tert*-butyl alcohol and a solution of 0.5 mM BPY/0.2 M *tert*-butyl alcohol, under the same conditions (400 °C/30 MPa) and the same flow rate (5 mL/min). For the MV^{2+} solution, the typical absorption spectrum of $MV^{\bullet+}$ is observed at λ_{max} = 605 nm, but λ_{max} for the radiolysis of BPY is 530 nm (a pulse radiolysis study on BPY in SCW will be published elsewhere). So, if the pyrolysis of MV^{2+} occurred, the shape of the spectrum observed would be different from that of $MV^{\bullet+}$, especially within the wavelength range 500−600 nm. We have compared the absorption spectrum of $MV^{\bullet+}$ in Figure 2 with the spectrum at room temperature, but no deformation of the spectrum in this region was observed. Another example is shown in the inset of Figure 3a; after normalization, the shape of the spectrum at 380 °C is almost the same as that at low temperatures. Figure 3b shows pressure-dependent absorption spectra of $MV^{\bullet+}$ recorded at 400 °C. It is clear that the shape of the spectrum remains almost the same under these conditions. Although it is expected that the MV^{2+} is no longer a dissociated ion but must be ion paired with the counterions (Cl^-) in low-density supercritical water, this experimental result shows no significant change in spectral properties (shape and peak position). One possibility is that a hydrated electron can react with the ion pair of methyl viologen, and the electron adduct has almost the same spectrum as $MV^{\bullet+}$. Therefore, we can conclude that the concentration of MV^{2+} does not change notably in the cell and MV^{2+} can be used as a scavenger in pulse radiolysis up to 400 °C provided that the flow rate is high enough (≥5 mL/min).

3.2. Estimation of $\{G(e_{aq}^-) + G(OH) + G(H)\}$ and $G(H)$ Using MV^{2+}/NaCOOH. As mentioned above, in the MV^{2+}/NaCOOH scavenging system, the three transient species (e_{aq}^-, OH, and H) are converted to $MV^{\bullet+}$. Figure 3a shows the absorption spectra of the $MV^{\bullet+}$ cation radical at different temperatures, from room temperature to 200 °C for the MV^{2+}/NaCOOH system and also a spectrum at 380 °C using MV^{2+}/*tert*-Butyl alcohol. The absorbances have been calibrated by density, that is, divided by density. It is clear that the peak positions do not change. If we normalize the absorbance at 605 nm to 1, as shown in the inset of Figure 3a, then the shape of the absorption spectra changes only very slightly, even at 380 °C. This is a very important feature because it implies that the absorption coefficient of $MV^{\bullet+}$ changes only slightly with the temperature, just as reported by Shiraishi, et al.[24] in the study of the same chemical system by a γ-radiolysis method up to 200 °C. Based on this assumption, for temperatures above 200 °C, the absorption coefficient can be obtained by extrapolation.

Thus from Figure 3a, we can deduce $\{G(e_{aq}^-) + G(OH) + G(H)\}$ at different temperatures according to equations (i) and (iii), as shown in Figure 4 (open circles, using a solution of 0.5 mM MV^{2+}/10 mM NaCOOH). In the figure, the lines are drawn according to the empirical equations provided by Elliot.[7] Our experimental result apparently agrees very well with the reported data. This strongly suggests that the scavenging system behaves as expected and the experimental method is reliable.

With the MV^{2+}/NaCOOH scavenging system, we have also tried to estimate $G(H)$ up to 200 °C. Since there is more than

SCHEME 1. Thermal Decomposition of Methyl Viologen

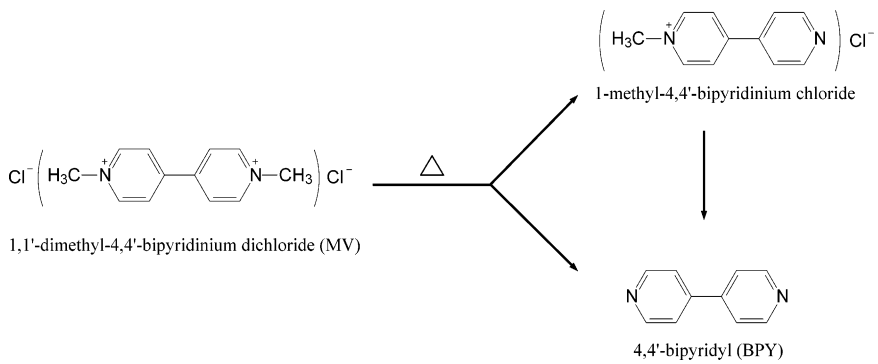

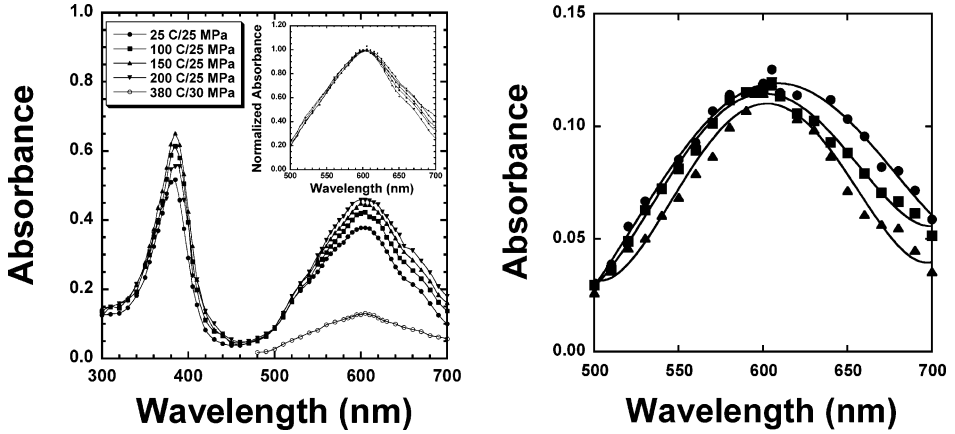

Figure 3. (a) Temperature-dependent absorption spectrum of methyl viologen cation radical $MV^{\bullet+}$ obtained by pulse radiolysis of an aqueous solution containing 0.5 mM MV^{2+} and 10 mM NaCOOH for temperatures from 25 to 200 °C, and 0.5 mM MV^{2+}/0.2 M *tert*-butyl alcohol for 380 °C. Dose: 30 Gy, optical path: 1.5 cm. Inset: the absorbancies at 605 nm are normalized to 1. (b) Absorption spectra of $MV^{\bullet+}$ at 400 °C: (●) 30 MPa; (■) 35 MPa; (▲) 40 MPa.

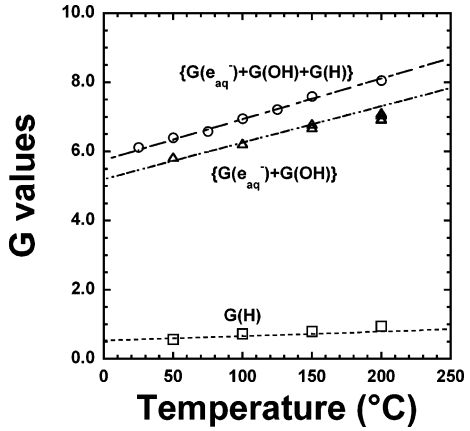

Figure 4. *G* values at various temperatures estimated by pulse radiolysis of two aqueous solutions: (○) 0.5 mM MV^{2+}/10 mM NaCOOH and (△) 0.5 mM MV^{2+}/1 mM NaCOOH. Their difference corresponds to G(H) (□). The dashed lines are plotted according to Elliot.[7]

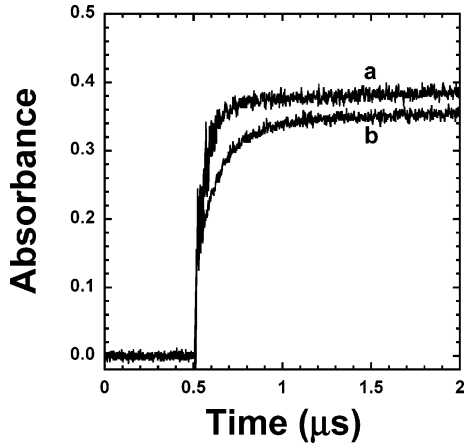

Figure 5. Time profiles at 605 nm of the formation of $MV^{\bullet+}$ after pulse radiolysis of (a) 0.5 mM MV^{2+}/10 mM NaCOOH and (b) 0.5 mM MV^{2+}/1 mM NaCOOH.

one order of magnitude difference between the rate constants of the reaction of MV^{2+} with the OH and the H radical (see reactions 3 and 4), when different concentrations of NaCOOH are used, as shown in Figure 5, for the higher concentration ([NaCOOH] = 10 mM), the formation of $MV^{\bullet+}$ quickly reaches a plateau while for the lower concentration ([NaCOOH] = 1 mM), the evolution takes much longer because the contribution

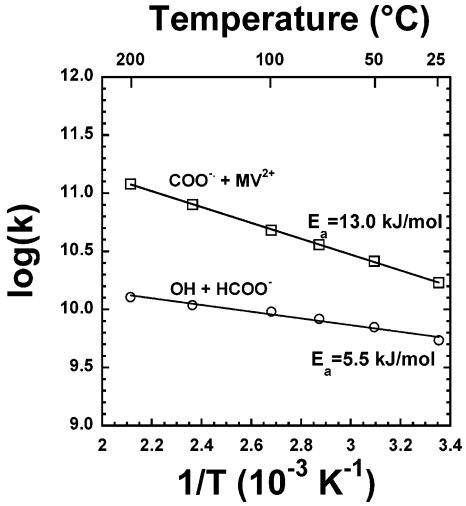

Figure 6. Arrhenius plots of reactions 3 and 5.

of the H radical is still negligible. Therefore, the difference of the $G(MV^{\bullet+})$ corresponds to G(H). Based on this method, G(H) can be roughly estimated. Figure 4 shows the result at different temperatures. It is comparable with the reported values.[7]

We have attempted to estimate the temperature dependence of the rate constants k_3 and k_5. For that, instead of bubbling with argon, N_2O gas was used. Under these conditions, the hydrated electron produced by the electron beam reacts quickly with N_2O to form an OH radical:[31]

$$e_{aq}^- + N_2O \rightarrow N_2 + OH + OH^- \quad k_6 = 9.1 \times 10^9\ M^{-1}s^{-1} \tag{6}$$

The ratio of $[MV^{2+}]/[HCOO^-]$ was varied and the formation time profiles of $MV^{\bullet+}$ at 605 nm were measured at each ratio. Kinetics simulation software FACSIMILE (MCPA Software Ltd.) was used to fit the signals by appropriately adjusting k_3 and k_5. The rate constants k_3 and k_5 at each measured temperature were obtained in this way, and the Arrhenius plots shown in Figure 6 were obtained. Both reactions show a fairly good linear relationship between log(k) and 1/T. Reaction 3 has an activation energy of 5.5 kJ/mol, which is comparable with the value reported by Elliot et al.,[37] 4.0 kJ/mol. Reaction 5 has an activation energy of 13.0 kJ/mol, which is close to diffusion-controlled if its high rate constant (1×10^{10} $M^{-1}s^{-1}$) at room temperature is taken into consideration.

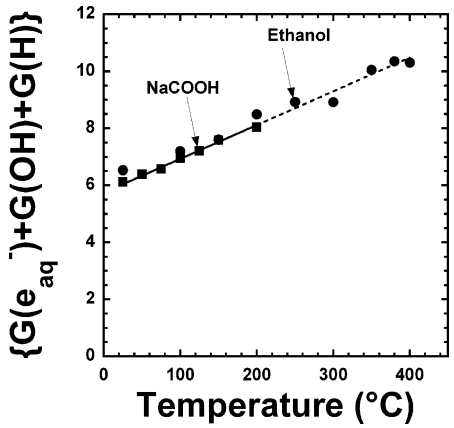

Figure 7. $\{G(e_{aq}^-) + G(OH) + G(H)\}$ as a function of temperature. (■) 0.5 mM MV^{2+}/10 mM NaCOOH; (●) 0.5 mM MV^{2+}/0.2 M ethanol. From room temperature to 350 °C, the pressure is 25 MPa while it is 30 MPa at 380 and 400 °C.

Although MV^{2+}/NaCOOH is a very convenient system, it can be used only up to 200 °C. Above 200 °C, even without irradiation, a blue color was observed while the solution passed through the high-temperature cell. This blue color corresponds to the formation of $MV^{\bullet+}$. The same phenomenon was also observed by Shiraishi et al.[24]

3.3. Estimation of $\{G(e_{aq}^-) + G(OH) + G(H)\}$ Using MV^{2+}/Ethanol. It is well-known that some alcohol radicals formed by H-atom abstraction possess reducing properties:[33]

$$OH + ROH \rightarrow H_2O + {}^{\bullet}ROH \quad (7)$$

$$H + ROH \rightarrow H_2 + {}^{\bullet}ROH \quad (8)$$

The OH and H radical are converted to the reducing radical $^{\bullet}$ROH. For example, the standard reduction potentials of $CH_3{}^{\bullet}CHOH$ and $(CH_3)_2{}^{\bullet}COH$ are −1.1 V and −1.5 V,[34] respectively. The reduction potential of $MV^{2+}/MV^{\bullet+}$ was reported to be −0.448 V.[35] Therefore, for these alcohols, after reaction with the OH and H radical, their radicals will reduce MV^{2+} to $MV^{\bullet+}$, and the $G(MV^{\bullet+})$ is equal to the sum of the G value of e_{aq}^-, OH, and H. From the viewpoint of the reduction potential, it seems that 2-propanol could be one of the best choices. However, experiments done with 2-propanol indicate a problem of thermal stability. From the kinetic signals, at elevated temperatures, the contribution to the reduction of MV^{2+} by the alcohol radical $(CH_3)_2{}^{\bullet}COH$ becomes smaller and smaller with increasing temperature, and in supercritical conditions it is likely that only the reduction by a hydrated electron could be observed.

Therefore, we selected ethanol because it has been proven to be fairly stable. Without an oxidizer, at 430 °C, almost no decomposition product could be detected by a Raman spectroscopy method.[36] Figure 7 shows that $\{G(e_{aq}^-) + G(OH) + G(H)\}$ increases with temperature up to 350 °C at a pressure of 25 MPa. The G value obtained by this scavenging system is comparable with that obtained from MV^{2+}/NaCOOH and the reported data up to 200 °C as well as those extrapolated to higher temperatures by Elliot.[7] However, it is likely that $\{G(e_{aq}^-) + G(OH) + G(H)\}$ measured by 0.5 mM MV^{2+}/0.2 M ethanol is slightly higher. This could be due to the higher concentration of ethanol we used. Since the rate constants of the reaction of ethanol with OH and the H radical are 1.9×10^9 $M^{-1}s^{-1}$ and 1.7×10^7 $M^{-1}s^{-1}$ (Buxton et al.[31]) to scavenge the H radical efficiently, a high concentration (0.2 M) was used for ethanol; this would cause too high a scavenging capacity ($k \times [S] = 3.8 \times 10^8$ s^{-1}) and ethanol will scavenge the OH radical in the spur even at room temperature.

Figure 8a shows the temperature dependence of $\{G(e_{aq}^-) + G(OH) + G(H)\}$ at two fixed densities, 0.35 and 0.50 g/cm^3, within the temperature range 375−400 °C. It is clear that $\{G(e_{aq}^-) + G(OH) + G(H)\}$ decreases with increasing temperature at a given density, and the lower the density the higher value of this G value. The latter can be seen very clearly in Figure 8b, which shows the variation with density of $\{G(e_{aq}^-) + G(OH) + G(H)\}$ at 400 °C. At relatively higher densities, 0.35−0.52 g/cm^3, (corresponding to a pressure range of 30−40 MPa), the G value changes slightly with density; at lower pressures, especially at 25 MPa (density: 0.167 g/cm^3), it suddenly increases to about 22. The same phenomenon was also observed for $G(e_{aq}^-)$ and we will discuss this density effect in the next section.

3.4. Estimation of $G(e_{aq}^-)$ Using MV^{2+}/*tert*-Butyl Alcohol. In the presence of *tert*-butyl alcohol, OH and H are scavenged, and only the hydrated electron reacts with MV^{2+}. The temperature dependence of the rate constant of reaction 2 was measured up to 350 °C. To do this, two HPLC pumps were employed. One was for loading a stock solution of 100 μM MV^{2+}/0.2 M *tert*-butyl alcohol while another was for pumping pure water containing 0.2 M *tert*-butyl alcohol. The pH of the two solutions was adjusted to 8.3 at room temperature. Under these conditions, we were able to change the concentration of MV^{2+} by adjusting the flow rates of the two HPLC pumps. The pulse duration of the electron beam was 2 ns and the dose per pulse was about 8 Gy. Although a higher dose would improve the S/N ratio of the transient absorption signals, to satisfy the pseudo-first-order condition, a higher concentration of MV^{2+} would be required. This would result in very fast decay at higher temperature, which would be beyond the time resolution of our current detection system. On the other hand, too small a dose would be unfavorable because the absorbance of the hydrated electron decreases significantly at elevated temperature and this causes a poor S/N ratio. Figure 9 shows the Arrhenius plot obtained for the reaction between the hydrated electron and MV^{2+} up to 350 °C at a constant pressure of 25 MPa. The decay of the hydrated electron at 800 or 900 nm was monitored. At a given temperature, the kinetics of hydrated electron decay with 3−5 concentrations of MV^{2+} were measured and at every concentration at least four signals were obtained for averaging. The rate constant at room temperature determined by this method was 8.1×10^{10} $M^{-1}s^{-1}$. The good agreement with the reported value[31] 8.3×10^{10} $M^{-1}s^{-1}$ supports the reliability of the method. The solid line shows a linear fit for temperatures up to 300 °C. From the slope, an activation energy of 21.6 kJ/mol is obtained. This value is slightly higher than that obtained by Elliot et al.,[37] 17.9 kJ/mol, which was measured up to 200 °C with a fixed concentration (10.5 μM) of MV^{2+} and with saturation pressures, and as stated by the authors, the rate constants were corrected for the natural decay of the hydrated electron in absence of solute. However, the results are considered to be in agreement within experimental error.

The yield of the hydrated electron was estimated using a deaerated solution containing 0.5 mM MV^{2+}/0.2 M *tert*-butyl alcohol. Figure 10 shows the variation of $G(e_{aq}^-)$ with temperature at a constant pressure of 25 MPa. Obviously, from room temperature to 300 °C, $G(e_{aq}^-)$ increases almost linearly with temperature. This agrees fairly well with previously reported data.[7,9] However, when the temperature is higher than 300 °C, $G(e_{aq}^-)$ decreases with temperature and then increases sharply at 400 °C. According to Jay-Gerin et al.,[11] who performed Monte

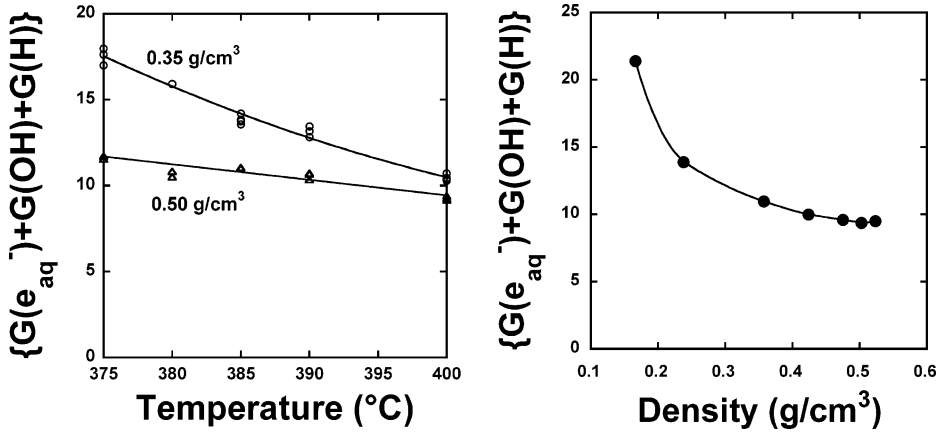

Figure 8. (a) $\{G(e_{aq}^-) + G(OH) + G(H)\}$ as a function of temperature at two fixed densities: (○) 0.35 g/cm^3 and (△) 0.50 g/cm^3. (b) $\{G(e_{aq}^-) + G(OH) + G(H)\}$ as a function of density at 400 °C.

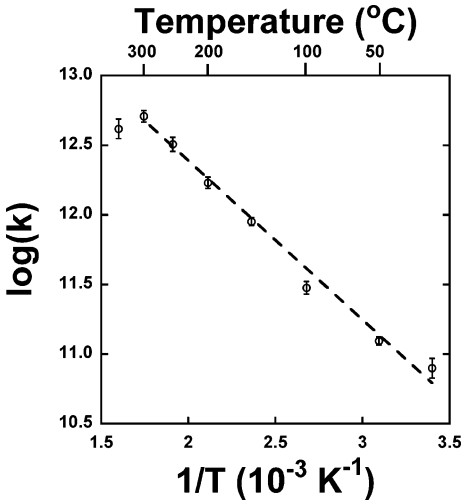

Figure 9. Arrhenius plot of the reaction between hydrated electron and MV^{2+}.

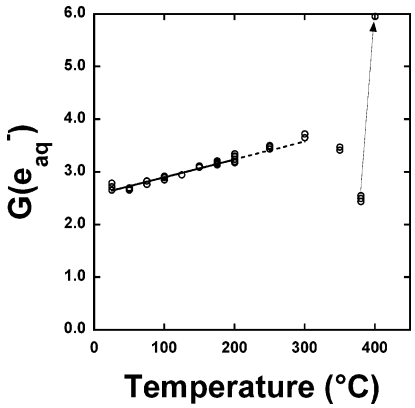

Figure 10. $G(e_{aq}^-)$ as a function of temperature at 25 MPa obtained by pulse radiolysis of a solution of 0.5 mM MV^{2+} and 0.2 M *tert*-butyl alcohol.

Carlo simulations to calculate the temperature dependence of $G(e_{aq}^-)$ at elevated temperature (≤325 °C), one of the reasons for the increase of this G with temperature is that many important spur reactions are not diffusion controlled and therefore have rate constants that increase less steeply with temperature than do the diffusion coefficients of the individual species; under such conditions, these reactions occur less as the temperature increases, which leads to more hydrated electrons being able to escape from the spurs. The reason for the decrease above 300 °C is much more complicated. It is due to density effects, as we will see below.

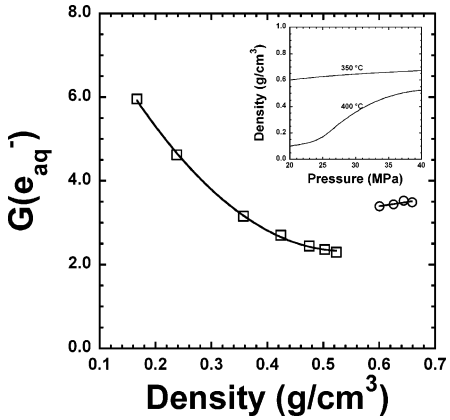

Figure 11. Density effects on $G(e_{aq}^-)$ at (○) 350 °C and (□) 400 °C. Inset: density as a function of pressure.

Figure 11 shows $G(e_{aq}^-)$ at 350 and 400 °C as a function of density. At 350 °C, within the density range we measured, $G(e_{aq}^-)$ is almost constant, or if anything, increases slightly with density. However, at 400 °C, $G(e_{aq}^-)$ changes dramatically with density; it is about 2.2 and 5.8 at $\rho = 0.50$ and 0.167 g/cm^3, respectively. It should be noted that, in the pressure range used (that is, from 25 to 40 MPa), the density at 400 °C largely depends on pressure. At 350 °C, the dependence of density on pressure is not so remarkable, as shown in the inset of Figure 11.

To elucidate the density effects on $G(e_{aq}^-)$ in supercritical conditions, we fixed the density at 0.20, 0.25, 0.35, and 0.50 g/cm^3 and measured the $G(e_{aq}^-)$ from 375 to 400 °C in intervals of 5 °C, as shown in Figure 12. At a given density, $G(e_{aq}^-)$ decreases with increasing temperature while at a given temperature it decreases with increasing density.

In Figure 13a, we assemble most of the experimental data on $G(e_{aq}^-)$ and draw them as a 3D plot to show $G(e_{aq}^-)$ as a function of density and pressure. The $G(e_{aq}^-)$ based on the equation by Elliot[7] is also plotted along the saturation line (where the liquid and vapor phases are in equilibrium). And for easier reading, we also plot the pressure vs. density plane of our experimental data together with the isothermal curves, as shown in Figure 13b. From these plots, one can see that there is almost no pressure (or density) effect at temperatures lower than 300 °C. However, above 300 °C, especially in supercritical conditions, the pressure effect is very significant. Clearly there is a valley around a density of 0.5 g/cm^3. In the authors' group,

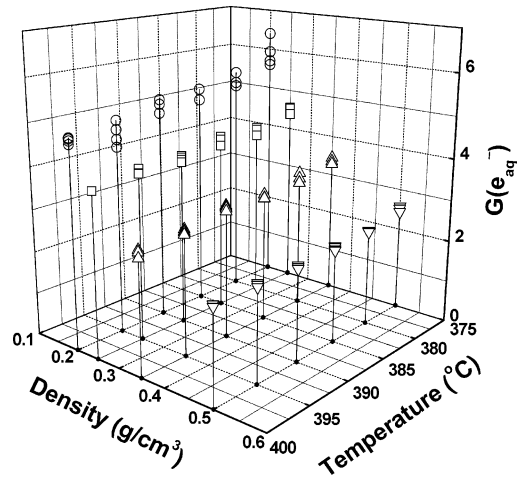

Figure 12. 3D plot of $G(e_{aq}^-)$ as a function of density and temperature in supercritical water. (○) 0.20 g/cm^3, (□) 0.25 g/cm^3, (△) 0.35 g/cm^3, and (▽) 0.50 g/cm^3.

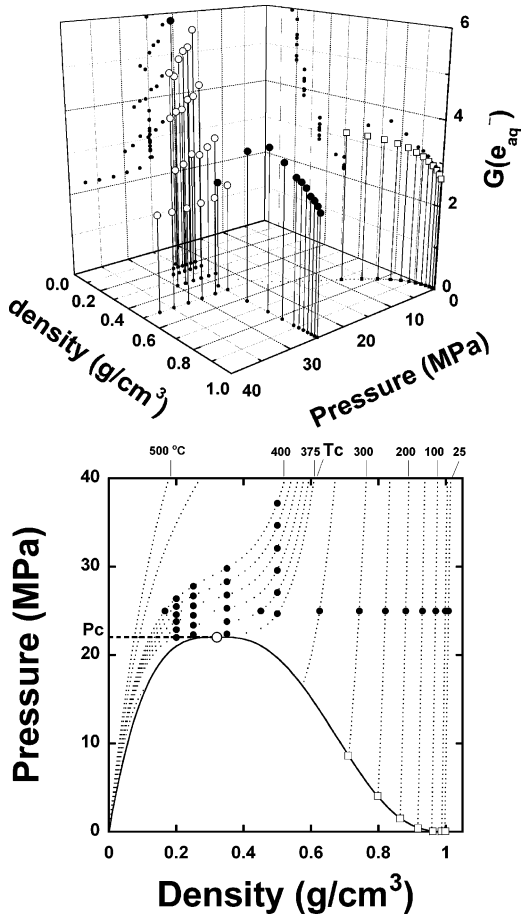

Figure 13. (a) 3D plot of $G(e_{aq}^-)$ as a function of density and pressure. (●) data correspond to Figure 10; (○) data correspond to Figure 12; (□) according to the equations in Elliot.[7] (b) *XY* plane of 13a with addition of the isothermal curves. The open circle is the critical point.

a study on the γ-radiolysis of benzophenone also shows a very similar density effect on the radiolytic yield of benzophenone decomposition under supercritical conditions.[38]

It is common knowledge that the yield of a hydrated electron is related to its escape probability from geminate−ion recombination. Physical properties such as dielectric constant, density, etc. might affect the escape probability. As a matter of fact, these physical properties are also density dependent under supercritical conditions.[39] However, we find that no single physical property could perfectly explain the existence of the valley. For example, at a given density, with increasing temperature, the dielectric constant decreases. According to Onsager's theory,[40] the Onsager length $r_c \equiv e^2/(4\pi\epsilon_0\epsilon k_B T)$ (e: magnitude of charge of electron; ϵ_0: permittivity of vacuum; ϵ: relative permittivity (dielectric constant) of the medium; k_B: Boltzman constant; and T: temperature), will increase, so that the escape probability, $\phi = \exp(-r_c/r_0)$, decreases. Here r_0 stands for the thermalization length. This is consistent with the experimental results. However, at a given temperature of supercritical water, the dielectric constant increases with pressure; therefore the escape probability should increase and higher $G(e_{aq}^-)$ should be observed. Evidently, this is contrary to the experimental results. Recently, in pulse radiolytic studies of supercritical CO_2, Dimitrijevic et al.[41,42] found that the amount of $C_2O_4^+$ formed is not proportional to the CO_2 density. They argued that the density effects on r_c and r_0 go in opposite directions and the large yields at low density can be explained by large values of r_0.

We suppose that the density effect would be related to the local density effect. In fact, the so-called 'local density augmentation', a greatly enhanced density of solvent molecules compared to the bulk fluid density near to or below the critical density, has been investigated for some years in supercritical fluids.[5,43] In the neighborhood of critical points, that is, from subcritical (350 °C) to 380 °C ($T/T_c \approx 1.1$), water is largely compressible and it is well-known that near the critical point, there exists a clustering effect of water molecules, while the hydrogen bond network is broken. With increasing temperature, the density becomes lower; therefore, the 'barrier' of solvent becomes less important and higher G values are observed. Obviously, this is also true when the density decreases at a given temperature, as we can see in Figure 12. Cline et al.[22] have reported the effect of density on the rate constants at 380 °C. In their studies of the reactions of hydrated electrons with the hydrophobic reactants O_2 and SF_6, a dramatic drop of rate constants between 0.55 and 0.45 g/cm^3 was observed, as well as an increase in the rate constants at a lower density (0.1 g/cm^3). They argued that whereas hydrophilic ions attract water molecules, hydrophobic molecules repel water, thereby producing a 'potential of mean force' barrier for the reactions. A large solvent barrier is not present in the high-density liquid phase. At much lower density the rate constant increases again, presumably because there are fewer water molecules to present a barrier. But in our case, the MV^{2+} is a cation and is hydrophilic. Even if the rate constant between a hydrated electron and MV^{2+} decreases at this density, a decrease by a factor of four (as reported by Cline, et al.[22]) would be unlikely to have much effect on $G(e_{aq}^-)$.

It is worth noting that $G(e_{aq}^-)$ is rather high at lower density, for example, at 400 °C/25 MPa (which corresponds to a density of 0.167 g/cm^3), its value is close to 6. This value could be too high from the standpoint of the *W*-value (the average energy required to produce a pair of ions in the medium) and with respect to the reported values of the initial yield of hydrated electrons, varying from 4.0 to 4.8, according to different groups.[44−49] Since in the scavenging system MV^{2+}/*tert*-butyl alcohol the reduction of MV^{2+} should be mainly due to hydrated electrons (it seems unlikely that a H radical could be able to reduce MV^{2+} because the reduction potential of $MV^{2+}/MV^{\bullet+}$ is −0.448 V[35]), it is suspected that at least part of the hydrated electron could come from the equilibrium of H_{aq} and e_{aq}^-,

$$H_{aq} \rightleftharpoons e_{aq}^- \qquad (9)$$

In fact, Han, et al.[50] have discussed the mechanism of this interconversion and pointed out that the H atom can effectively disproportionate and leave the electron to become hydrated within the H atom solvent cage. In addition, the recent work of Cline, et al.,[22] has shown that the ratio of G_H/G_e greatly depends on the density, especially in supercritical conditions. In low-density supercritical water, the initial yield of H atoms could be five or six times the yield of hydrated electrons. As mentioned above, in our experiments we used 0.2 M *tert*-butyl alcohol to scavenge OH radicals and H atoms. At room temperature, the reported rate constant of the reaction between *tert*-butyl alcohol and a H atom is 1.7×10^5 $M^{-1}s^{-1}$[51] or 1.15×10^6 $M^{-1}s^{-1}$,[52] while the rate constant of the reaction between MV^{2+} and a H atom is 6×10^8 $M^{-1}s^{-1}$.[32] Apparently, *tert*-butyl alcohol is unable to scavenge all H atoms before they react with MV^{2+}. Although no data are available for the rate constants of these two reactions in supercritical water, a similar situation could exist, that is, part of H atoms react with MV^{2+} to form $(MVH^{\bullet})^{2+}$. It is also speculated that this H adduct could dissociate to produce $MV^{\bullet+}$. This would explain our observation of a higher yield of hydrated electrons.

In Figure 13, it is also interesting that at a given density, the lowest temperature always has a higher $G(e_{aq}^-)$ value. From Figure 13b, it is likely that this is because the conditions are much closer to gas phase. The rather high $G(e_{aq}^-)$ and $\{G(e_{aq}^-) + G(OH) + G(H)\}$ at lower density is probably due to an increase of radiation-induced dissociation of water molecules, approaching the radiolysis of water vapor. As shown in Figure 8, $\{G(e_{aq}^-) + G(OH) + G(H)\}$ at 400 °C/25 MPa is as high as about 22. It can be assumed that every H_2O^+ (equal amount of electrons) generates an OH radical through the ion−molecular reaction. In addition, the fragmentation of H_2O results in equal amounts of OH and H radicals. Since the value of $G(e_{aq}^-)$ under the same condition was determined as about 6, this means the yield of water fragmentation is about 10. In a study of the kinetic behavior of hydrated electrons (in D_2O) at elevated temperatures (up to 390 °C and probably with a maximum pressure of 250 atm), Michael et al.[53] found that an assumption of $G(D) = 10$ and $G(OD) = 12.5$ resulted in a better fitting of the kinetic signals. They argued that the radiolysis of water above 300 °C approaches that of the vapor. In fact, $G(OH) = 8.2$ and $G(H) = 7.2$,[27,54,55] and $G(OH) = G(H) = 11$[56,57] for water vapor have been reported.

4. Conclusion

Methyl viologen aqueous solutions in the presence of various scavengers can be used to evaluate the yields of the primary products of water radiolysis decomposition to 400 °C. At a pressure of 25 MPa, $G(e_{aq}^-)$ increases with temperature up to 300 °C, then decreases to 380 °C and sharply increases at 400 °C. $\{G(e_{aq}^-) + G(OH) + G(H)\}$ increases with temperature up to 350 °C at 25 MPa. The dissociation of water becomes more important at lower pressure in supercritical water. In supercritical conditions, both $G(e_{aq}^-)$ and $\{G(e_{aq}^-) + G(OH) + G(H)\}$ depend not only on temperature but also on density, which is very different from the situation at room temperature or even at elevated temperatures. The density effect has been supposed to be partly due to the changes of water density, especially local density in supercritical conditions, but the nature of the effect should be investigated by further experiments or computer simulation.

Acknowledgment. We are grateful to T. Ueda, K. Yoshii, and Prof. M. Uesaka for their technical assistance in experiments. This work was supported by the Ministry of Education, Culture, Sports Science and Technology (MEXT), Japanese Government, as a "Fundamental R&D program on water chemistry of supercritical pressure water under radiation field."

References and Notes

(1) Savage, P. E. *Chem. Rev.* **1999**, *99*, 603.
(2) Tester, J. W.; Cline, J. A. *Corrosion*, **1999**, *55*, 1088.
(3) Schmieder, H.; Abeln, J. *Chem. Eng. Technol.* **1999**, *22*, 903.
(4) Bröll, D.; Kaul, C.; Krämer, A.; Krammer, P.; Richter, T.; Jung, M.; Vogel, H.; Zehner, P. *Angew. Chem., Int. Ed.* **1999**, *38*, 2999.
(5) Kajimoto, O. *Chem. Rev.* **1999**, *99*, 355.
(6) Oka, Y. *Proceedings 1998 Frederic Joliot Summer School in Reactor Physics*; August 1998, Caderache, France; pp 240−259 and references cited herein.
(7) Elliot, A. J. *Rate Constants and G-Values for the Simulation of the Radiolysis of Light Water over the Range 0−300 °C*; AECL-11073, COG-1994, 94−167.
(8) Elliot, A. J.; Ouellette, D. C.; Stuart, C. R. *The Temperature Dependence of the Rate Constants and Yields for the Simulation of the Radiolysis of Heavy Water*; AECL-11658, COG-96−390−1, 1996.
(9) Buxton, G. V. High-Temperature Water Radiolysis. In *Radiation Chemistry: Present Status and Future Trends*, Jonah, C. D. Rao, B. S. M., Eds.; Elsevier: Tokyo, 2001, 145−162.
(10) Swiatla-Wojcik, D.; Buxton, G. V. *J. Phys. Chem.* **1995**, *99*, 11464.
(11) Meesungnoen, J.; Jay-Gerin, J. P.; Filali-Mouhim, A.; Mankhetkorn, S. *Can. J. Chem.* **2002**, *80*, 767.
(12) Ferry, J. L.; Fox, M. A. *J. Phys. Chem. A* **1998**, *102*, 3705.
(13) Ferry, J. L.; Fox, M. A. *J. Phys. Chem. A* **1999**, *103*, 3438
(14) Wu, G.; Katsumura, Y.; Muroya, Y.; Li, X.; Terada, Y. *Chem. Phys. Lett.* **2000**, *325*, 531.
(15) Wu, G.; Katsumura, Y.; Muroya, Y.; Lin, M.; Morioka, T. *J. Phys. Chem. A*, **2001**, *105*, 4933.
(16) Katsumura, Y.; Wu, G.; Lin, M.; Muroya, Y.; Morioka, T.; Terada, Y.; Li, X. *Res. Chem. Intermed.* **2001**, *27*, 753.
(17) Wu, G.; Katsumura, Y.; Muroya, Y.; Lin, M.; Morioka, T. *J. Phys. Chem. A*, **2002**, *106*, 2430.
(18) Mostafavi, M.; Lin, M.; Wu, G.; Katsumura, Y.; Muroya, Y. *J. Phys. Chem. A*, **2002**, *106*, 3123.
(19) Wu, G.; Katsumura, Y.; Lin, M.; Morioka, T.; Muroya, Y. *Phys. Chem. Chem. Phys.* **2002**, *4*, 3980.
(20) Bartels, D. M.; Cline, J. A.; Jonah, C. D.; Takahashi, K. *Abstr. Pap. Am. Chem. Soc.* **2001**, *222*, U217, Part 2.
(21) Takahashi, K.; Bartels, D. M.; Cline, J. A.; Jonah, C. D. *Chem. Phys. Lett.* **2002**, *357*, 358.
(22) Cline, J. A.; Takahashi, K.; Marin, T. W.; Jonah, C. D.; Bartels, D. M. *J. Phys. Chem. A*, **2002**, *106*, 12260.
(23) Marin, T. W.; Cline, J. A.; Takahashi, K.; Jonah, C. D.; Bartels, D. M. *J. Phys. Chem. A*, **2002**, *106*, 12270.
(24) Shiraishi, H.; Buxton, G. V.; Wood, N. D. *Radiat. Phys. Chem.* **1989**, *33*, 519.
(25) Elliot, A. J.; Chenier, M. P.; Oullette, D. C. *J. Chem. Soc., Faraday Trans.* **1993**, *89*, 1193.
(26) Buxton, G. V.; Stuart, C. R. *J. Chem. Soc., Faraday Trans.* **1995**, *91*, 279.
(27) Spinks, J. W. T.; Woods, R. J. *An Introduction to Radiation Chemistry*; John Wiley & Sons: New York, 1990, p 260.
(28) Mulazzani, Q. G.; D'Angelantonio, M.; Venturi, M.; Hoffman, M. Z.; Rodgers, M. A. J. *J. Phys. Chem.* **1986**, *90*, 5347.
(29) Farrington, J. A.; Ebert, M.; Land, E. J.; Fletcher, K. *Biochim. Biophys. Acta* **1973**, *314*, 372.
(30) Patterson, L. K.; Small, R. D., Jr.; Scaiano, J. C. *Radiat. Res.* **1977**, *72*, 218.
(31) Buxton, G. V.; Greenstock, C. L.; Helman, V. P.; Ross, A. B. *J. Phys. Chem. Ref. Data* **1988**, *17*, p 513.
(32) Solar, S.; Solar, W.; Getoff, N.; Holcman, J.; Sehested, K. *J. Chem. Soc., Faraday Trans.* **1984**, *80*, 2929.
(33) Buxton, G. V. In *Radiation Chemistry: Principles and Applications*. Farhataziz, Rodgers, M. A. J., Eds.; VCH Publishers: New York, 1987, p 343.
(34) Asmus, K. D.; Möckel, H.; Henglein, A. *J. Phys. Chem.* **1973**, *77*, 1218.
(35) Wardman, P. *J. Phys. Chem. Ref. Data*. **1989**, *18*, 1637.
(36) Rice, S. F.; Croiset, E. *Ind. Eng. Chem. Res.* **2001**, *40*, 86.
(37) Elliot, A. J.; McCracken, D. R.; Buxton, G. V.; Wood, N. D. *J. Chem. Soc., Faraday Trans.* **1990**, *86*, 1539.
(38) Miyazaki, T.; Katsumura, Y.; Morioka, T. et al., to be published.
(39) Please refer to IAPWS Web site: http://www.iapws.org.
(40) Mozumder, A. *Fundamentals of Radiation Chemistry*; Academic Press: New York, Tokyo, 1999.

(41) Dimitrijevic, N. M.; Bartels, D. M.; Jonah, C. D.; Takahashi, K. *Chem. Phys. Lett*. **1999**, *309*, 61.
(42) Dimitrijevic, N. M.; Takahashi, K.; Bartels, D. M.; Jonah, C. D.; Trifunac, A. D. *J. Phys. Chem.* **2000**, *104*, 568.
(43) Akiya, N.; Savage, P. E. *Chem. Rev.* **2002**, *102*, 2725.
(44) (*a*) Wolff, R. K.; Bronskill, M. J.; Aldrich, J. E.; Hunt, J. W. *J. Phys. Chem.* **1973**, *77*, 1350. (*b*) Hunt, J. W.; Wolff, R. K.; Bronskill, M. J.; Jonah, C. D.; Hart, E. J.; Matheson, M. S. *J. Phys. Chem.* **1973**, *77*, 425. (*c*) Wolff, R. K.; Aldrich, J. E.; Penner, T. L.; Hunt, J. W. *J. Phys. Chem*. **1975**, *79*, 210. (*d*) Hunt, J. W. *Adv. Radiat. Chem*. **1976**, *5*, 185.
(45) Jonah, C. D.; Matheson, M. S.; Miller, J. R.; Hart, E. J. *J. Phys. Chem*. **1976**, *80*, 1267.
(46) Pimblott, S. M.; LaVerne, J. A.; Bartels, D. M.; Jonah, C. D. *J. Phys. Chem*. **1996**, *100*, 9412.
(47) (*a*) Sumiyoshi, T.; Katayama, M. *Chem. Lett*. **1982**, 1887. (*b*) Sumiyoshi, T.; Tsugaru, K.; Yamada, T.; Katayama, M. *Bull. Chem. Soc. Jpn*. **1985**, *58*, 3073.
(48) Bartels, D. M.; Cook, A. R.; Mudaliar, M.; Jonah, C. D. *J. Phys. Chem*. A, **2000**, *104*, 1686.
(49) Muroya, Y.; Lin, M.; Wu, G.; Iijima, H.; Yoshii, K.; Ueda, T.; Katsumura, Y. *Radiat. Phys. Chem.*, in press.
(50) Han, P.; Bartels, D. M. *J. Phys. Chem*. **1992**, *96*, 4899.
(51) Smaller, B.; Avery, E. C.; Remko, J. R. *J. Chem. Phys.* **1971**, *55*, 2414.
(52) Wojnárovits, L.; Takács, E.; Dajka, K.; Emmi, S. S.; Russo, M.; D'Angelantonio, M. *Radiat. Phys. Chem.* **2004**, *69*, 217.
(53) Michael, B. D.; Hart, E. J.; Schmidt, K. H. *J. Phys. Chem.* **1971**, *75*, 2798.
(54) Dixon, R. S. *Radiat. Res. Rev.* **1970**, *2*, 237.
(55) Boyd, A. W.; Willis, C.; Miller, O. A. *Can. J. Chem*. **1973**, *51*, 4048.
(56) Firestone, R. F. *J. Am. Chem. Soc.* **1957**, *79*, 5593.
(57) Baxendale, J. H. *J. Am. Chem. Soc*. **1964**, *86*, 516.